



INTERNATIONAL ATOMIC ENERGY AGENCY  
UNITED NATIONS EDUCATIONAL, SCIENTIFIC AND CULTURAL ORGANIZATION



INTERNATIONAL CENTRE FOR THEORETICAL PHYSICS  
34100 TRIESTE (ITALY) - P.O. B. 500 - MIRAMARE - STRADA COSTIERA 11 - TELEPHONE: 2940-1  
CABLE: CENTRATOM - TELEX 620222-1

H4.SMR/381-9

COLLEGE ON ATOMIC AND MOLECULAR PHYSICS:  
PHOTON ASSISTED COLLISIONS IN ATOMS AND MOLECULES

(30 January - 24 February 1989)

HIGHLY EXCITED ATOMS:  
CREATION & ANNIHILATION

Lecture 2

J. LEVENTHAL

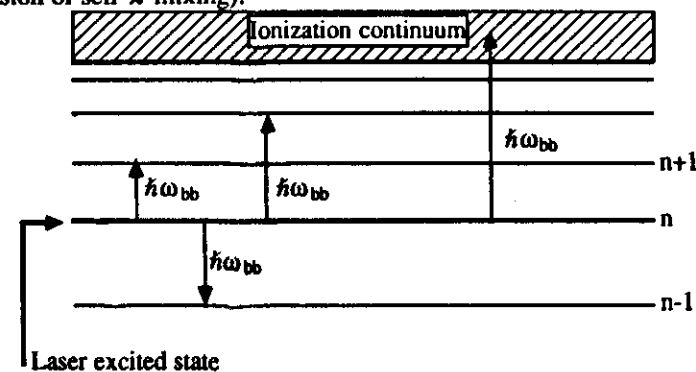
University of Missouri - St. Louis  
Dept. of Physics  
St. Louis, Missouri  
U.S.A.

### OUTLINE FOR LECTURE #2

1. Effects of blackbody radiation (continued).
2. Experiments that demonstrate the effects of blackbody radiation.
3. Heavy body collisions
4. Molecular potential energy curves.
5. Laser induced effects.

### EFFECTS OF BLACKBODY RADIATION ON RYDBERG ATOMS

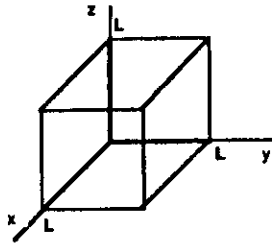
We have seen that the 300 K blackbody spectrum has sufficient intensity of radiation at frequencies appropriate for photoexcitation, stimulated emission and photoionization. We have even seen that photoionization can be used as a means of detection and to make deductions about other phenomena (recall our discussion of self- $\lambda$ -mixing).



We now consider this phenomenon in more detail by examining photoexcitation. We begin our discussion with a closer look at blackbody radiation. For more details see:

*The quantum theory of light* by R. Loudon (Clarendon Press; Oxford)

We limit the region of space by imagining a cavity in which the radiation is confined. We consider a cubic cavity of side  $L$ , the walls of which are perfectly conducting so the tangential component of the  $\mathbf{E}$  field vanishes at the boundaries.



The electric field must satisfy the wave equation

$$\nabla^2 \mathbf{E} = \frac{1}{c^2} \frac{\partial^2 \mathbf{E}}{\partial t^2}$$

and  $\nabla \cdot \mathbf{E} = 0$ . The solution that satisfies the boundary conditions is

$$\begin{aligned} E_x(\mathbf{r}, t) &= E_x(t) \cos(k_x x) \sin(k_y y) \sin(k_z z) \\ E_y(\mathbf{r}, t) &= E_x(t) \sin(k_x x) \cos(k_y y) \sin(k_z z) \\ E_z(\mathbf{r}, t) &= E_x(t) \sin(k_x x) \sin(k_y y) \cos(k_z z) \end{aligned}$$

The wavevector  $\mathbf{k}$  has components  $k_x = \pi n_x / L$ , etc.  $n_i = 0, 1, 2, \dots$

The allowed values of  $\mathbf{k}$  can be plotted as a lattice of points in three dimensions with spacing  $\pi/L$ . Since each lattice point is surrounded by an empty volume of  $(\pi/L)^3$  the number of field modes having a magnitude of their wavevector between the values  $k$  and  $k + dk$  is

$$\frac{1}{8} [4\pi k dk] [\pi/L]^{-3} \times 2$$

The density  $\rho_k dk$  of field modes is the number of modes per unit volume having their wavevector in the specified range and is

$$\rho_k dk = k^2 dk / \pi^2$$

Using  $\omega = ck$  we can convert this into an expression for the density  $\rho_\omega d\omega$  of modes having their frequency between  $\omega$  and  $\omega + d\omega$

$$\rho_\omega d\omega = \omega^2 d\omega / c^3 \pi^2$$

The total average field energy can be shown to be

$$\frac{1}{2} \int_{\text{cavity}} \epsilon_0 |\mathbf{E}(\mathbf{r}, t)|^2 dV$$

Now we introduce the Planck hypothesis. The field  $\mathbf{E}(t)$  satisfies the harmonic oscillator equation which, if treated quantum mechanically, leads to quantized energy level given by

$$E_n = (n + 1/2) \hbar \omega \quad \text{with} \quad n = 1, 2, 3 \dots$$

These allowed values of the electromagnetic energy of the mode may thus be equated to the classical result above

$$\frac{1}{2} \int_{\text{cavity}} \epsilon_0 |\mathbf{E}(\mathbf{r}, t)|^2 dV = E_n = (n + 1/2) \hbar \omega$$

Now the Boltzmann factor

$$P_n = \frac{\exp(-E_n / k_B T)}{\sum_n \exp(-E_n / k_B T)}$$

gives the probability  $P_n$  that the mode oscillator is thermally excited to the  $n$ th excited state. The denominator is a geometric series, the sum of which is given by

$$\sum_{n=0}^{\infty} U^n = \frac{1}{1 - U} \quad \text{where} \quad U = \exp(-E_n / k_B T)$$

The mean number  $\bar{n}$  of photons excited in the field mode at temperature  $T$  is therefore

$$\begin{aligned}\bar{n} &= \sum_n n P_n = (1 - U) \sum_n n U^n \\ &= (1 - U) U \frac{\partial}{\partial U} \left\{ \sum_n U^n \right\} \\ &= (1 - U) U \frac{\partial}{\partial U} \left\{ \frac{1}{1 - U} \right\} = U / (1 - U)\end{aligned}$$

so that

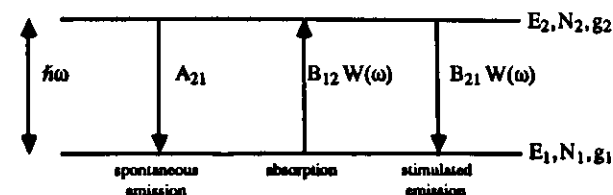
$$\bar{n} = \frac{1}{\exp(\hbar\omega/k_B T) - 1}$$

Combining the density of field modes with the mean energy per mode we obtain the mean energy density  $\bar{W}_T(\omega)d\omega$  of the radiation in these modes at temperature  $T$ .

$$\bar{W}_T(\omega)d\omega = \bar{n}\hbar\omega\rho_\omega d\omega = \bar{n} \frac{\hbar\omega^3}{\pi^2 c^3} = \frac{\hbar\omega^3}{\pi^2 c^3} \frac{d\omega}{\exp(\hbar\omega/k_B T) - 1}$$

This is the Planck law for the radiative energy density  $\bar{W}_T(\omega)$ .

Returning now to the Einstein relations



The three basic kinds of radiative processes.

The rates of change of  $N_1$  and  $N_2$  are given by

$$\frac{dN_1}{dt} = -\frac{dN_2}{dt} = N_2 A_{21} - N_1 B_{12} \bar{W}(\omega) + N_2 B_{21} \bar{W}(\omega)$$

and in thermal equilibrium the level populations are constant so that

$$N_2 A_{21} - N_1 B_{12} \bar{W}(\omega) + N_2 B_{21} \bar{W}(\omega) = 0$$

or

$$\bar{W}_T(\omega) = \frac{A_{21}}{(N_1/N_2) B_{12} - B_{21}}$$

The level populations are related by Boltzmann's law

$$N_1/N_2 = (g_1/g_2) \exp(-\hbar\omega/k_B T)$$

where  $k_B$  is the Boltzmann constant. We have

$$\bar{W}_T(\omega) = \frac{A_{21}}{(g_1/g_2) \exp(\hbar\omega/k_B T) B_{12} - B_{21}}$$

Comparing this to Planck's law we see that

$$[g_1/g_2] B_{12} = B_{21}$$

and

$$[\hbar\omega^3/\pi^2 c^3] B_{21} = A_{21}$$

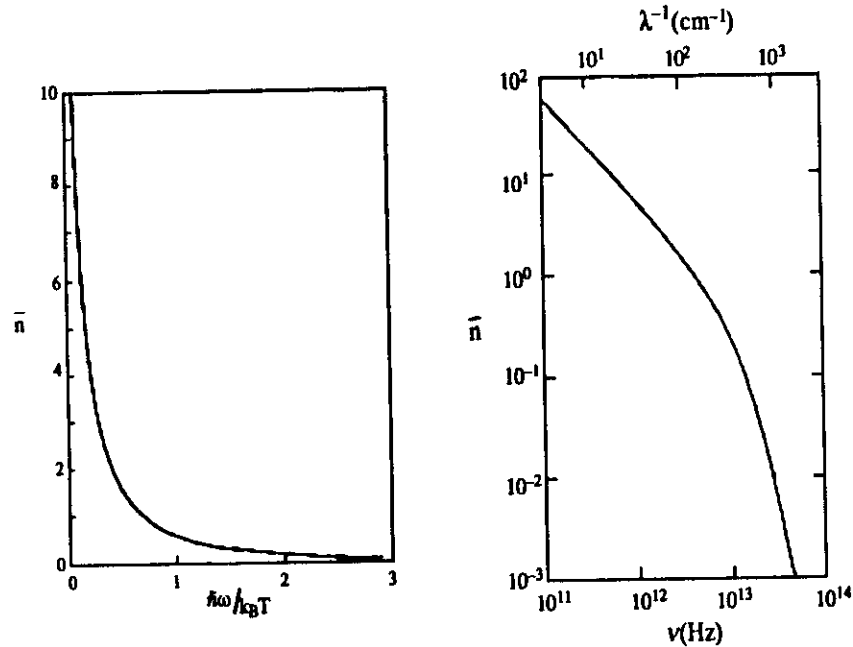
which shows the relationship between the three Einstein coefficients. Since Planck's law can also be written  $\bar{W}_T(\omega) = \hbar\omega^3/\pi^2 c^3$  we have the rate of stimulated emission due to blackbody radiation is given by

$$K_{21} = B_{21} \bar{W}(\omega) = A_{21} \bar{n}$$

Furthermore, the rate of absorption is given by

$$K_{12} = (g_1/g_2)B_{12}W(\omega) = A_{21}\bar{n}$$

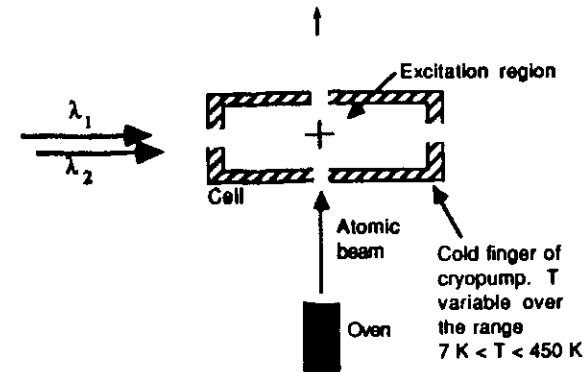
Examining  $\bar{n}$  graphically



we see why blackbody radiation can have such an important effect on a state-selected sample of Rydberg atoms for which the transitions are  $\sim 10^{11}$  Hz.

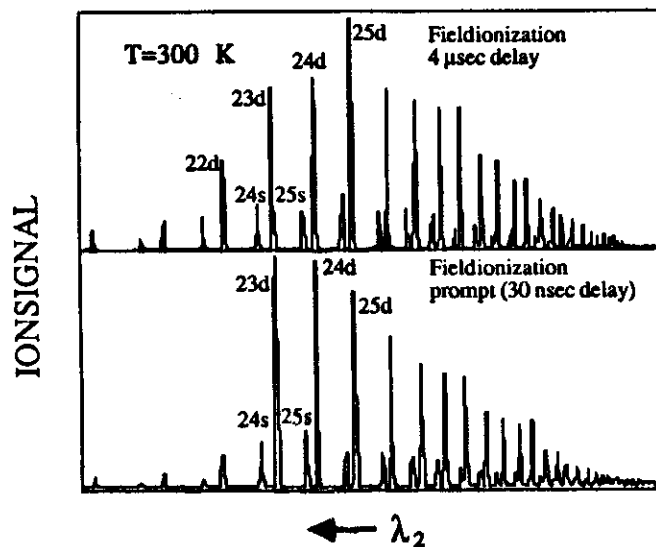
Also,  $k_B T$  for 300 K is  $\sim 1/40$  eV  $\approx 200$   $\text{cm}^{-1}$ , but  $\Delta E$  for  $n=20$  is  $\sim 30$   $\text{cm}^{-1}$ . Therefore  $\hbar\omega/k_B T \approx 0.15$  for which  $\bar{n}$  is  $\sim 6$ . For lower lying states  $\bar{n}$  is much smaller (see graphs above).

We have constructed apparatus identical to that described earlier. We have however mounted the cell that defines the excitation region on the "cold finger" of a cryogenic pump so that we may control the ambient temperature of the surroundings over the approximate range  $7 \text{ K} < T < 450 \text{ K}$ . Essentially it is the same apparatus as described earlier, but the significant technological change is the addition of the cryogenic feature.

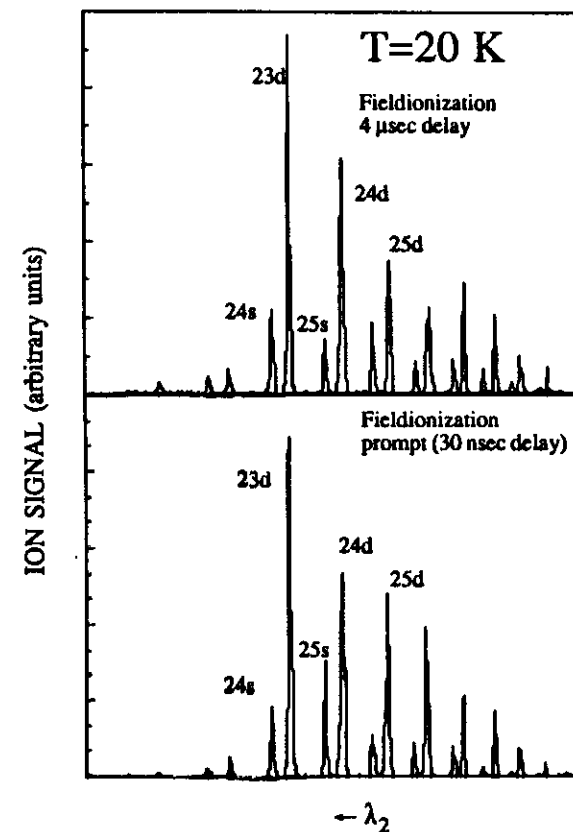


The field ionization plates are omitted from the figure, but are in the apparatus.

We now examine some data acquired using this apparatus.

TYPICAL DATA ACQUIRED WITH THE  
THRESHOLD SET FOR  $n=23d$ 

"Deterioration" of the sharp threshold in the 4  $\mu\text{s}$  delay spectrum demonstrates that  $n$ -changing to higher  $n$ 's is occurring. Further, reduction of the peaks at  $n=23$  and 24, which are just above the threshold, in the 4  $\mu\text{s}$  delay spectrum clearly shows that  $n$ -changing to lower  $n$ 's is also occurring.

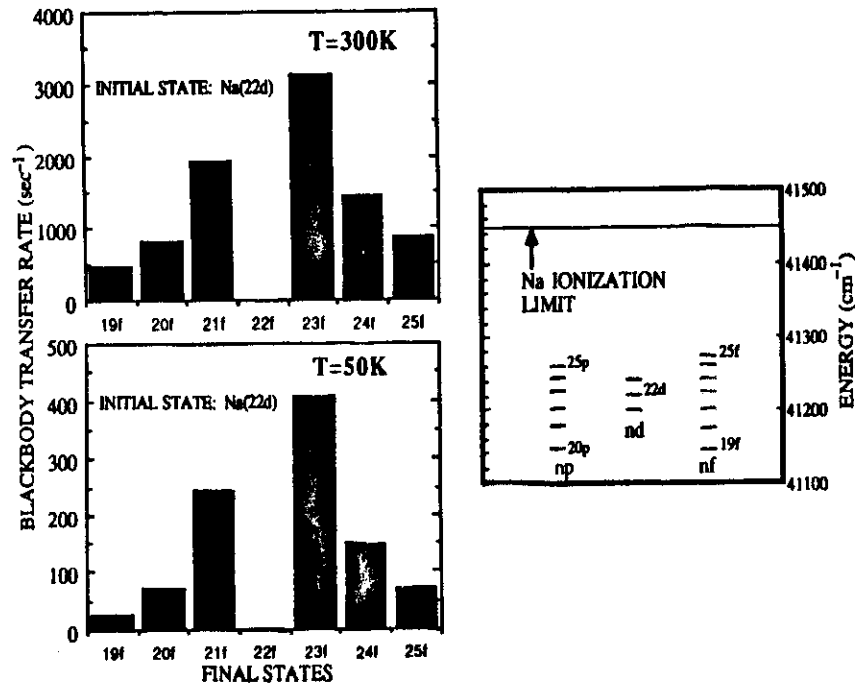


At this temperature there is little difference between the prompt and the delayed field ionization spectra. This indicates that  $n$ -changing has been virtually eliminated.

To quantitatively assess the validity of this conclusion we have computed blackbody induced transfer rates between states  $i$  and  $j$

$$K_{ij} = \bar{n} A_{ij}$$

using the method of Edmonds et al [J. Phys B 12, 2781 (1979)]. For transfer out of the 22d state of sodium to neighboring levels we have



Note that the ratios of the rates at the different temperatures remain roughly the same because  $\hbar\omega \ll k_B T$  for these temperatures. Therefore

$$\bar{n} = \frac{1}{\exp(\hbar\omega/k_B T) - 1} \approx \frac{1}{1 + (\hbar\omega/k_B T) + \dots - 1} \approx \frac{k_B T}{\hbar\omega}$$

## HEAVY BODY COLLISIONS

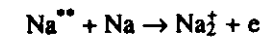
Because of the large size of Rydberg atoms they frequently have enormous cross sections for reaction with other atoms. We have already seen that  $\ell$ -mixing in collisions between sodium Rydberg atoms and ground state atoms has an enormous cross section,  $\sim 10^5 \text{ \AA}^2$ .

We now describe some collisional processes in which the products are different chemical species than the reactants.

We have REACTANTS  $\rightarrow$  PRODUCTS

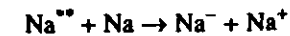
First we consider

Associative ionization



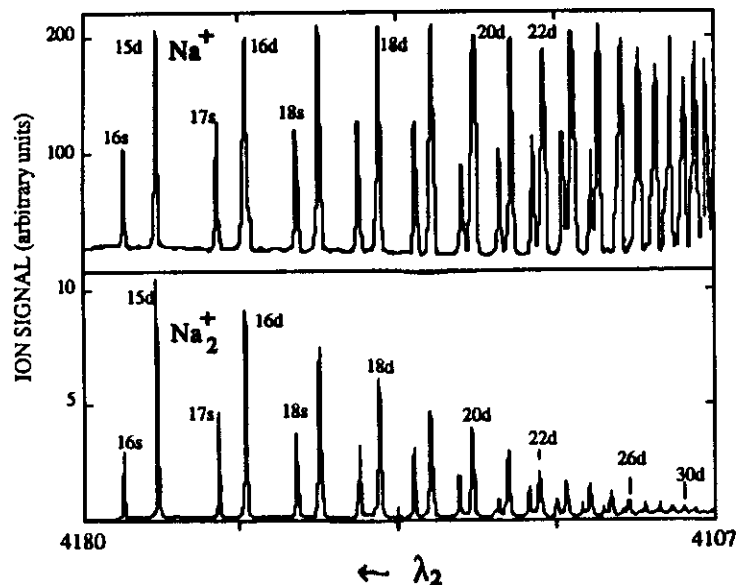
and

Ion-pair formation (electron transfer)



By adding a mass spectrometer to the apparatus we may distinguish between  $\text{Na}^+$  and  $\text{Na}_2^+$ . This mass spectrometer, in conjunction with a change of electrical polarity of the detector, permits us to isolate  $\text{Na}^-$  from other ions formed in the excitation region.

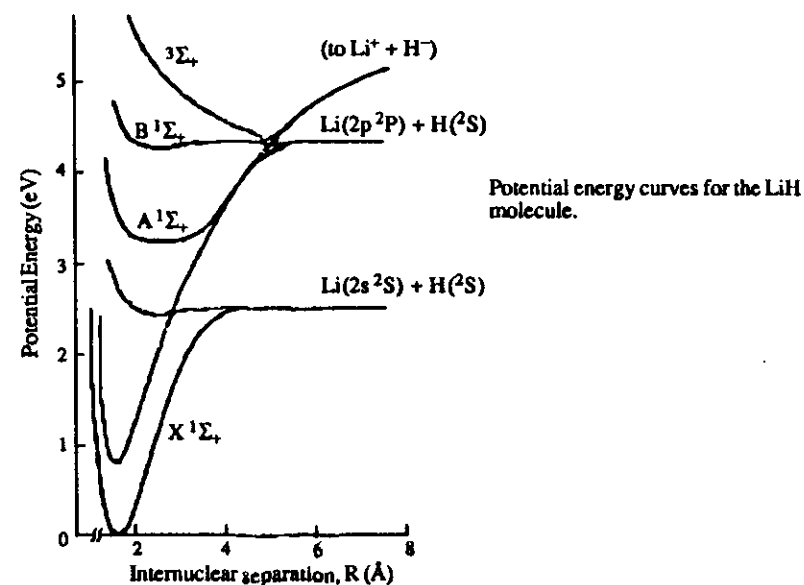
The spectrum in the top panel is simply a blackbody photoionization spectrum and serves to locate the wavelengths at which sodium Rydberg atoms are produced.



The lower spectrum is one taken with the mass spectrometer set to transmit only mass 46,  $\text{Na}_2^+$ . Note the decrease of the peaks heights with decreasing  $\lambda$ . This is more rapid than the  $n^{-3}$  characteristic of the production rate of the Rydberg atoms.

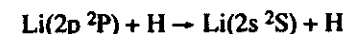
Before discussing these results we digress to discuss potential energy curves for diatomic molecules.

As the internuclear separation between two atoms decreases and their respective electron clouds overlap the potential energy of the two changes. If it decreases then a chemical bond can be formed, for example two H atoms form a bound  $\text{H}_2$  molecule. If it increases, as for example two ground state helium atoms, then no bond is formed. This is illustrated below for the LiH molecule.



Notice that a different set of curves result if one of the atoms is in an excited atomic state. Also, this picture is for a rotationless molecule. For nonzero angular momentum there is a barrier caused by the centrifugal term in the three dimensional potential,  $V(r)$ .

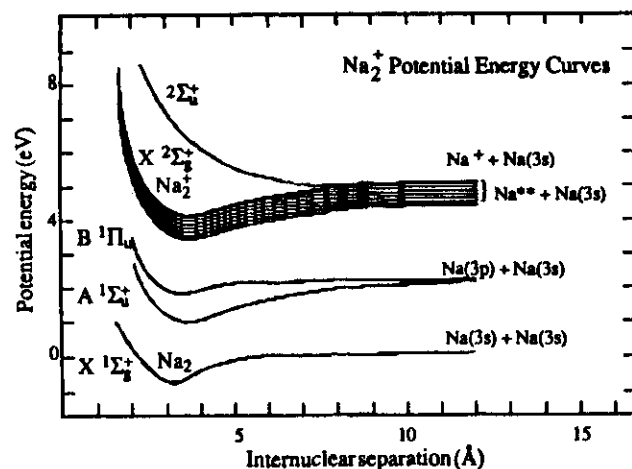
We may view an atomic collision as occurring along one of these curves. If a reaction occurs, then the colliding system "switches" to another curve. For example, using the curves above, suppose we have a collision between an excited Li atom and a ground state H atom that results in two ground state species. That is,



This quenching collision may be viewed as occurring along the upper curve, the entrance channel, and terminating along the lower curve, the exit channel. The  $\sim 2$  eV difference between these channels is taken up as kinetic energy of the product atoms.



Now we examine the potential energy curves relevant to  $\text{Na}^{**}\text{-Na}$  associative ionization.

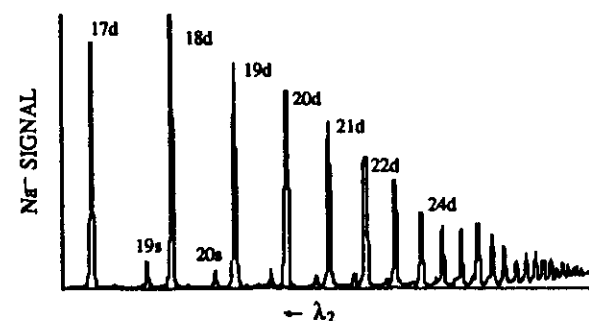


Because the Rydberg electron does not participate in the bonding that forms the highly excited diatomic molecule,  $\text{Na}_2^{**}$ , crossing from the entrance channel to the exit channel can easily be accomplished.

The Rydberg electron must carry off the extra energy as kinetic energy in order to stabilize the  $\text{Na}_2^{**}$ . Therefore this electron must "communicate" with the ion core and must have low angular momentum. High  $\ell$ -states do not penetrate the core. Since however the cross section for this  $\ell$ -mixing is roughly 3 orders of magnitude larger than the associative ionization cross section, the reactants for associative ionization are not state selected, but rather statistically  $\ell$ -mixed. This means that the higher the  $n$  value, the higher the proportion of states that are in high angular momentum states because the high angular momentum states are statistically favored, i.e.  $2\ell+1$  states per  $\ell$ -state.

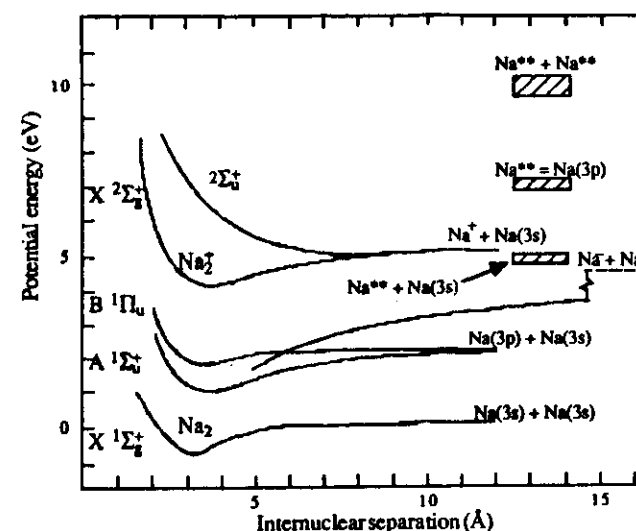
As  $n$  increases then the fraction of atoms in low angular momentum states decreases. This qualitatively accounts for the observed steep decrease in the associative ionization cross section with increasing  $n$ .

We have also observed  $\text{Na}^-$  from  $\text{Na}^{**}$ .

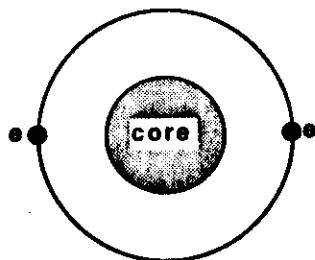


We were surprised however to find that at high values of  $n$  the ion pair formation occurs between two Rydberg atoms, rather than one Rydberg atom and one ground state atom. This was ascertained by performing laser power dependences. These dependences showed that two "blue" photons, and therefore two Rydberg atoms were required to produce a single  $\text{Na}^-$ .

The process is even more unusual when the entrance and exit channels are examined using potential energy curves.



Another possibility is the formation of a "planetary" negative ion.



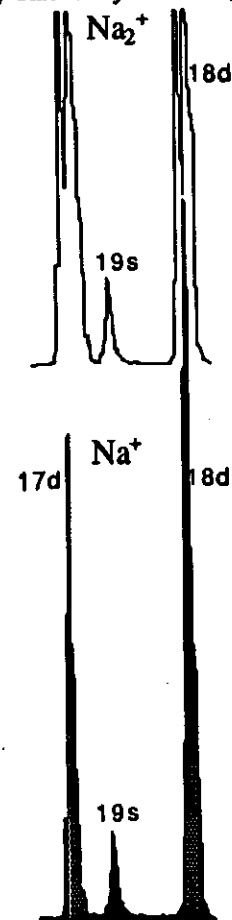
Can this "double Rydberg" structure exist?

Because the electronic orbital radius is large the e-e repulsion should be small.

This will be especially true if the electrons both have high  $\ell$ -values.

Unfortunately there does not seem to be a definitive experiment that will test for the existence for this  $[\text{Na}^{**}]^-$ .

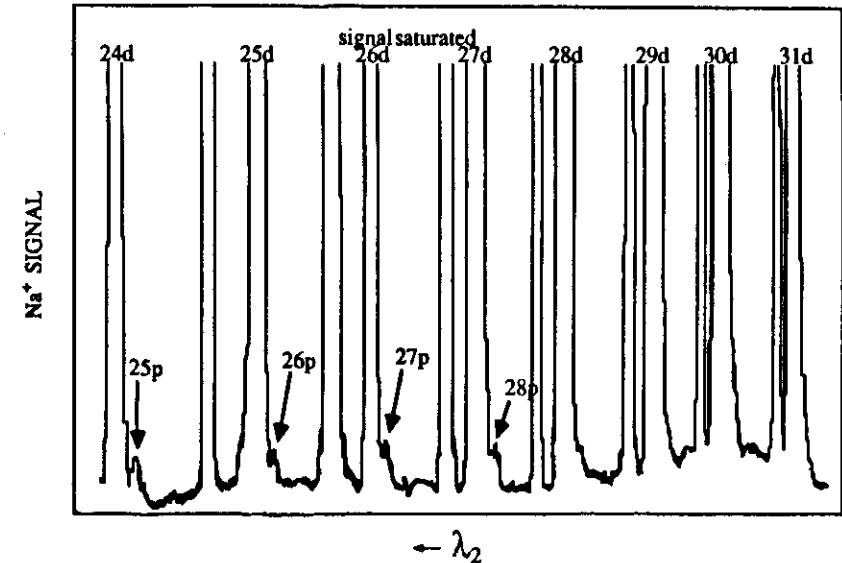
We now consider the effects of increasing the atomic density. It might be expected that higher signals of the products of  $\text{Na}^{**}\text{-Na}$  and  $\text{Na}^{**}\text{-Na}^{**}$  reactions would increase. That is not the case however as can be seen by examining the partial spectrum below. This spectrum was acquired with relatively high atom density,  $\sim 10^{14} \text{ cm}^{-3}$  which leads to a Rydberg atom density of  $\sim 10^{12} \text{ cm}^{-3}$ . Field ionization could not be used because electrical breakdown occurs at this density. The ion signal results from a combination of processes, for example, collisional ionization (both  $\text{Na}^{**}\text{-Na}$  and  $\text{Na}^{**}\text{-Na}^{**}$ ), ionization by blackbody radiation, etc.



Now however a different effect dominates. The obvious decrease in the  $\text{Na}_2^+$  signal at line center is accompanied by a sharp increase in the  $\text{Na}^+$  signal.

This effect is due to an avalanche of ionization of the Rydberg atoms by electron impact ionization. The ionization potential of say Na(17d) is  $\sim 13.6$  eV/ $n^2 \approx 0.04$  eV which is  $\sim kT$ . Therefore, any electrons present will likely have sufficient energy to ionize the Rydberg atoms. If there is a high concentration of Rydberg atoms, as there was when the above spectrum was acquired, then "seed" electrons would initiate a chain of ionization events. Each ionization adds another electron to the total, thus cascading the process. The seed electrons can come from a number of processes such as associative ionization, collisional ionization (product Na<sup>+</sup>), photoionization by blackbody radiation, etc. The dip in the Na<sub>2</sub><sup>+</sup> peak is due to a loss of reactant Rydberg atoms at line center.

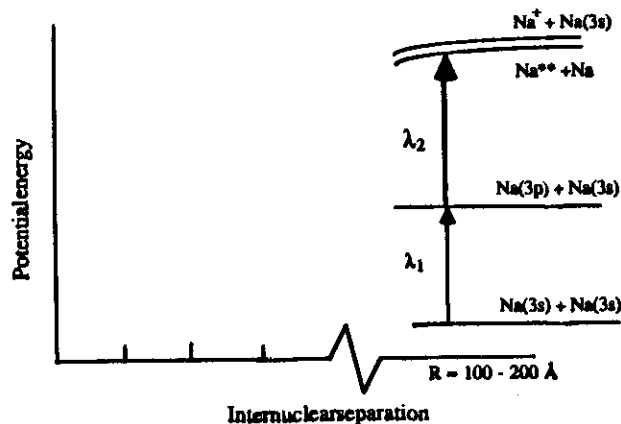
We now examine another interaction involving Rydberg atoms at relatively high density. This is an example of a "laser-induced reaction". The atomic selection rule (the Laporte rule)  $\ell \rightarrow \ell \pm 1$  requires production of only ns and nd states from the Na(3p) intermediate state in the  $3s \rightarrow 3p \rightarrow n\ell$  excitation scheme. Upon careful inspection of spectra taken at atomic density  $\sim 10^{14}$  cm<sup>-3</sup> we find very small peaks at wavelengths corresponding to the forbidden  $3p \rightarrow np$  transitions. See C. E. Burkhardt et al, Phys. Rev. Lett. 57, 1562 (1986).



We have shown that the np peak heights depend quadratically upon the atom density, indicating that two sodium atoms are required for this excitation to occur. We have also shown that the peaks are not due to electric quadrupole transitions or to Stark mixing from stray fields.

The interaction responsible for permitting the "forbidden" transition is essentially the same as that responsible for  $\ell$ -mixing of laser-produced (state-selected) Rydberg atoms. The cross section for self- $\ell$ -mixing is of the order of the Rydberg geometric cross section. Therefore, we may regard the  $3p \rightarrow np$  excitation as one in which an  $\ell$ -mixing collision occurs in the presence of the exciting radiation. This radiation must of course be tuned to the wavelength of the  $3p$ - $np$  energy separation. Therefore, when the Na(3s) [actually Na(3p) could also be involved] is within the geometric cross section of the final state the wavefunction has actually acquired d (and higher  $\ell$ 's) character. The observed "forbidden" transition then actually occurs between the 3p initial state and the d component of the  $\ell$ -mixed final state, in accordance with the Laporte rule.

The excitation may also be viewed from a molecular point of view. We may regard the absorption of  $\lambda_2$  as occurring during a transitory collision between Na(3s) and Na(3p) [or between Na(3p) and Na(3p)]. In this picture we have broken the spherical symmetry that dictates the atomic selection rules, the Laporte rule in particular, and are now subject to the less restrictive molecular selection rules that are governed by cylindrical symmetry. The transition is allowed under molecular selection rules. The diagram below illustrates this picture.



The unique features of these data are the relatively narrow absorption profiles of the forbidden transition and the low laser power density at which the absorption occurs. Other "laser-induced" collision phenomena typically require laser power densities of  $\sim 1 \text{ MW}$ , but this effect was observed with laser power densities of  $\sim 1 \text{ kW}$ .

It is the enormous  $\ell$ -mixing cross section that allows observation of this effect with only modest laser power density. Further, the long-range nature of the  $\ell$ -mixing interaction leads to long-duration collisions and narrow absorption profiles. In fact, in our experiment, the observed widths are  $\sim 0.1 \text{ cm}^{-3}$ , which is comparable with the laser linewidth.

The occurrence of this "laser-induced" effect at atypically low laser power densities is an example of an extreme property of Rydberg atoms magnifying an effect that would be otherwise difficult, or in some cases impossible to observe.